Biochimica et Biophysica Acta 1818 (2012) 82–89

Contents lists available at SciVerse ScienceDirect

Biochimica et Biophysica Acta

journal homepage: www.elsevier.com/locate/bbamem

The role of the C-terminal region of pulchellin A-chain in the interaction with membrane model systems

Luis Fernando Reyes [a,1], Thatyane M. Nobre [a,1], Felippe J. Pavinatto [b], Maria E.D. Zaniquelli [c], Luciano Caseli [d], Osvaldo N. Oliveira Jr. [b], Ana Paula U. Araújo [a,*]

[a] Centro de Biotecnologia Molecular Estrutural, Instituto de Física de São Carlos, Universidade de São Paulo, PO Box 369, 13560-970 São Carlos, SP, Brazil
[b] Grupo de Polímeros Bernhard Gross, Instituto de Física de São Carlos, Universidade de São Paulo, PO Box 369, 13560-970 São Carlos, SP, Brazil
[c] Departamento de Química, Faculdade de Filosofia, Ciências e Letras de Ribeirão Preto, Universidade de São Paulo, Ribeirão Preto, SP, Brazil
[d] Instituto de Ciências Ambientais, Químicas e Farmacêuticas, Universidade Federal de São Paulo, Diadema, SP, Brazil

ARTICLE INFO

Article history:
Received 25 July 2011
Received in revised form 29 September 2011
Accepted 4 October 2011
Available online 12 October 2011

Keywords:
Ribosome inactivating protein
Langmuir monolayers
Pulchellin
Membrane interaction
PM-IRRAS

ABSTRACT

Pulchellin is a *R*ibosome *I*nactivating *P*rotein containing an A-chain (PAC), whose toxic activity requires crossing the endoplasmic reticulum (ER) membrane. In this paper, we investigate the interaction between recombinant PAC (rPAC) and Langmuir monolayers of dipalmitoyl phosphatidyl glycerol (DPPG), which served as membrane model. Three catalytically active, truncated PACs with increasing deletion of the C-terminal region, possessing 244, 239 and 236 residues (rPAC^{244}, rPAC^{239} and rPAC^{236}), were studied. rPAC had the strongest interaction with the DPPG monolayer, inducing a large expansion in its surface pressure–area isotherm. The affinity to DPPG decreased with increased deletion of the C-terminal region. When the C-terminal region was deleted completely (rPAC^{236}), the interaction was recovered, probably because other hydrophobic regions were exposed to the membrane. Using Polarization Modulated-Infrared Reflection Absorption Spectroscopy (PM-IRRAS) we observed that at a bare air/water interface rPAC comprised mainly α-helix structures, the C-terminal region had unordered structures when interacting with DPPG. For rPAC^{236} the α-helices were preserved even in the presence of DPPG. These results confirm the importance of the C-terminal region for PAC-ER membrane interaction. The partial unfolding only with preserved C-terminal appears a key step for the protein to reach the cytosol and develop its toxic activity.

1. Introduction

Pulchellin is a type 2 Ribosome Inactivating Protein (RIP) isolated from seeds of the *Abrus pulchellus* plant [1]. As a type 2 RIP, it comprises two polypeptide chains named PAC (pulchellin A-chain) and PBC (pulchellin B-chain), linked by a disulfide bond. PAC is a highly specific RNA *N*-glycosylase that inhibits protein synthesis by irreversible depurination of 28S RNA of the 60S ribosome subunit (both *in vivo* and *in vitro*), while PBC is a galactose-specific lectin [2]. Analogously to ricin and abrin, pulchellin displays strong cytotoxic effects on mammalian cells [3,4] at low protein concentrations. Pulchellin enters cells through lectin–carbohydrate interactions at the cell surface followed by endocytic uptake and subsequent retrograde transport [3]. For type 2 RIPs the toxic A-chain, after being reduced from its B-chain, enters the cell cytoplasm by exploiting the ER-associated protein degradation pathway (ERAD) [5,6]. In spite of the increasing evidence for this pathway, it is still unclear how the A-chain is recognized as "substrate" by the ERAD machinery for cytosol translocation. A-chains usually present a patch of hydrophobic amino acids near the C-terminus, which is exposed upon separation of the chains [7]. The exposure of this hydrophobic region in the ER lumen could probably facilitate the interaction of the A-chain with the ER membrane, leading to partial unfolding and the recognition of the protein as an ERAD substrate [7].

The role of the hydrophobic C-terminal of type 2 RIP A-chains has been evaluated by some groups. Simpson et al. [8] noted that the hydrophobic amino acid residues near the C-terminus of ricin toxic A-chain (RTA) are determinant for the protein–ER membrane interaction. Also, they verified that the mutation in this region of the protein reduced the cytotoxicity significantly without affecting the catalytic activity of RTA. Suhan et al. observed that a peptide derived from the hydrophobic patch of the Shiga-like toxin, a type 2 RIP, is inserted into the membrane [9]. Based on the conservation of the hydrophobic region among RIPs, it might be a general membrane–RIP interaction, at least during this traffic step. More recently, the RTA–lipid interaction was found to be triggered at physiological temperatures, involving the exposure of its non-polar path also at the C-terminal [10].

Since most studies have been carried out with RTA, we were motivated to investigate the interaction between recombinant Pulchellin A-chain (rPAC) [1] and membrane models. Here, we demonstrate that rPAC interacts with negatively charged phospholipids using Langmuir

* Corresponding author. Tel.: +55 16 3373 9875; fax: +55 16 3371 5381.
E-mail address: anapaula@ifsc.usp.br (A.P.U. Araújo).
[1] These authors contributed equally to the work.

0005-2736/$ – see front matter © 2011 Elsevier B.V. All rights reserved.
doi:10.1016/j.bbamem.2011.10.002

monolayers as membrane models. We investigate the role of the C-terminus region of pulchellin A-chain on the interaction with the membrane, using three truncated forms. From surface pressure–area isotherms, we infer that all proteins interact with the membrane model, but at different extensions depending on the deletion in the rPAC C-end. Dilational surface elasticity pointed to drastic effects on the lipid packing with the adsorption of the proteins, which reflects changes in the membrane fluidity. Furthermore, polarization-modulation infrared reflection-absorption spectroscopy (PM-IRRAS) showed that rPAC and its truncated form rPAC^{236}, with major deletion of the C-terminal region, interacts with the lipid monolayer via different secondary structures. Further evidence will be presented in support of the insertion of the A-chain C-terminal into ER membrane, which is a crucial step in the intoxication process.

2. Materials and methods

2.1. Cloning of rPAC and its truncated forms

Recombinant pulchellin A-chain (rPAC) and the three truncated forms at its C-terminal region (Fig. 1) (henceforth referred to as rPAC$^{236/239/244}$ respectively) were generated by PCR using the pulchellin cDNA isoform PII [4], accession number EU008736.1, as template. Specific primer sequences were the following: rPAC-forward (5′*CGGCTAGCGAGGACCGGCCCATTGAATTTAC*) and rPAC-reverse (5′ *CCTTCGAGTTAATTTGGCGGATTGCAGACAAAA*), including the restriction sites for *Nhe*I and *Xho*I, respectively. Reverse primers for C-end deletions also include the *Xho*I restriction site: rPAC^{244} (*5′AGCTCGAGTTAAAGCATCAATGCTAGAACTGC*); rPAC^{239} (*5′AGCTCGAGTTAAACTGCTAGAGTTGGGTGTGAC*); and rPAC^{236} (5′*AGCTCGAGTTAAGTTGGGTGTGACAAGGAATC*). Each reverse primer was combined with the rPAC-forward primer to produce the truncated sequences. PCR cycling conditions were: 94 °C, 5 min; 35 cycles at 94 °C, 2 min, 60 °C, 30 s and 72 °C, 1 min, and a final extension at 72 °C, 5 min. PCR products were cloned into the pGEM-T (Promega) vector and sequenced using an ABI Prism 377 automated DNA sequencer (Perkin Elmer) following the manufacturer's protocol. The target sequences were subcloned into pET28a(+) vector (Novagen), thus generating four constructs: pETPAC, pETPAC^{244}, pETPAC^{239}, and pETPAC^{236}). The recombinant proteins produced from all those constructs had a 6xHis-tag at its N-terminal end.

2.2. Expression and purification of the proteins

Escherichia coli BL21 (DE3) strain was transformed with the above described constructs and then grown in 5 mL LB (Luria–Bertani) medium supplied with kanamycin (50 μg L^{-1}) during 16 h at 37 °C and 250 rpm. Subsequently, the cultures were diluted (1:100) in a new medium (100 mL LB supplied with kanamycin), growing under the same conditions. Bacterial cultures were grown until reaching the optical density (OD_{600nm}) of 0.4–0.6 where protein expression was induced by the addition of 0.1 mM IPTG. Induced cell cultures were then incubated during 16 h, at 20 °C and 250 rpm. The cells were pelleted by centrifugation at 4 °C and the samples were processed for the purification step. Thus, cell lysis was performed by sonication (30 s with 20 mA pulses, repeated 10 times) and the soluble fractions were collected after centrifugation at 9000×*g* in a Sorvall RC5C, at 4 °C. The recombinant PAC and their truncated forms were purified by affinity chromatography, briefly described as follows. Soluble samples were loaded into a 5 mL Ni-NTA resin (QIAGEN) containing column, pre-equilibrated with buffer A (20 mM NaH_2PO_4/Na_2HPO_4, 5 mM imidazole, pH 7.4). Unbounded proteins were washed with approximately 10–15 column volumes of the same buffer. Protein elution was performed by adding increasing concentrations of imidazole (diluted in buffer A). Both expression and purification results were analyzed on SDS-PAGE 15% [11], as shown in Fig. 2. Once confirmed its purity grade, each protein sample was dialyzed against buffer A without imidazole. All protein samples were immediately used in the experiments or kept overnight at 4 °C.

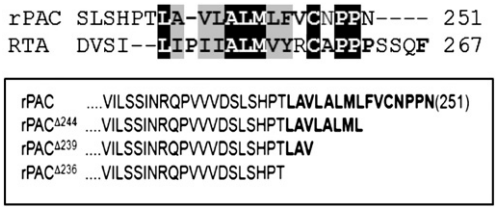

Fig. 1. Top: Clustal-W alignment result of RTA (P02879) and PAC showing the conserved patch of hydrophobic residues at C-terminus of rPAC and RTA. The identical and highly conserved amino acids have black and gray backgrounds, respectively. Bottom: C-terminal of rPAC and its truncated forms. Note that each mutant lacks some of its residues (bolded sequence when compared with rPAC. The nomination of each mutant corresponds to total residues of the protein. Thus, for instance rPAC$^{\Delta244}$ lacks seven residues of C-end and so on.

2.3. Depurination assay

All the recombinant proteins were assayed for the *in vitro* RNA *N*-glycosylase activity in the presence of rat liver ribosomes as described by Endo et al. [12] with minor modifications. Briefly, the reaction was performed as follows: 2 μL of (340 U/ml) Ribosome, 2 μL of Endo's buffer and sterile water up to 15 μL, then 5 μL of each protein was added to a 1.5 mL tube and thereafter incubated at 30 °C during 60 min. Once the reaction was completed, the RNA was purified using Trizol (Invitrogen) and the alcohol precipitation method according to the manufacturer's procedures. For aniline treatment, 10 μL of purified RNA (in sterile water) was mixed with 50 μL of aniline and the mixture was then incubated at 60 °C for 3 min. The reaction was immediately stopped by the addition of 30 μL of 7.5 M ammonium acetate and 180 μL of 100% ethanol, and it was frozen in dry-ice or −80 °C during several minutes. As negative control, PAC was substituted by sterile water and subjected to the same aniline treatment conditions. Recombinant PAC was used as a positive control. Aniline treated RNA was once again purified by alcohol precipitation. The results were analyzed through formamide-agarose and 7 M Urea-6% polyacrylamide electrophoresis to check the presence of the typical Endo's fragment.

2.4. Far-UV circular dichroism (CD) measurements

The CD spectra of the proteins in buffer solution (phosphate buffer 20 mM, pH 7.4) at concentration of 0.1 mg mL^{-1} were recorded from 190 to 250 nm with a JASCO J-715 spectropolarimeter (Jasco Instruments, Tokyo, Japan), as an average of 16 scans using a 0.1 cm path length cylindrical quartz cuvette, at 25 °C.

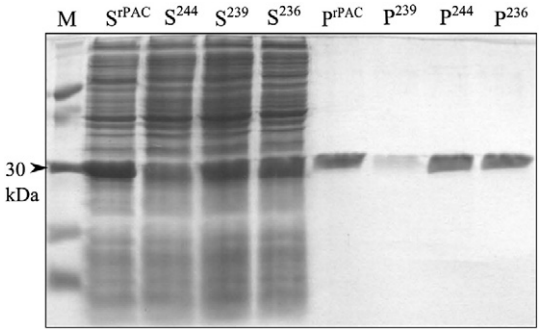

Fig. 2. Expression and purification analysis of rPAC and its C-terminus truncated forms. SDS-PAGE 15% showing (S) soluble fraction after cell lyses and (P) purified protein for rPAC, rPAC$^{\Delta244}$, rPAC$^{\Delta239}$ and rPAC$^{\Delta236}$ constructs; (M) corresponds to molecular weight marker.

2.5. π–A isotherms

Langmuir monolayers were formed by spreading a lipid solution over aqueous subphase containing phosphate buffer 20 mM, pH 7.4. The surface tension of the buffer solution was 73 mN m^{-1}. MilliQ-Plus™ water, resistivity 18.2 MΩ cm^{-1}, pH~5.5 was employed for preparing all buffer solutions. Dipalmitoyl phosphatidyl-glycerol (DPPG) solutions were prepared in chloroform:methanol (4:1), while dipalmitoyl phosphatidyl-choline (DPPC) was dissolved in pure chloroform. The surface pressure–area (π–A) isotherms were performed in a mini-KSV Langmuir trough equipped with a surface pressure sensor (Wilhelmy method) and housed in a class 10,000 clean room. π–A isotherms were obtained upon monolayer compression using movable barriers with a speed of 5 $Å^2$ $molecule^{-1}$ min^{-1}. Initially, a Langmuir trough with total capacity of 35 mL was filled with buffer solution and then the lipid was spread at the air–water interface to render an initial area per lipid molecule of ca. 135 $Å^2$. After solvent evaporation (20 min), an aliquot of the protein was injected in the subphase and compression was performed after measuring the adsorption kinetics at a low lipid surface density (with an initial surface pressure close to zero).

2.6. Interaction between the protein and DPPG at membrane lipid packing

Measurements of adsorption kinetics of the protein at the biomembrane lipid packing were carried out with the pendant drop method with axisymmetric drop shape analysis, using an automatic contact-angle-tensiometer OCA-20, from Dataphysics, Germany [13]. A DPPG solution of ca. 10^{-4} mol L^{-1} was gently touched on the surface of a reduced size drop, which was formed by buffer solution, with or without protein. The drop was then rapidly expanded up to a pre-determined drop area to yield a surface pressure of ca. 30 mN m^{-1}, which corresponds to the biomembrane lipid packing [14]. Subsequent changes in surface pressure due to protein adsorption or alterations in the lipid conformation were plotted against time. The dynamic surface elasticity data were obtained after the surface tension reached a constant value, by using a periodic drop oscillation of amplitude 0.1 mm (relative area variation $\Delta A/A$ of 5.5%) and frequency of 1.0 Hz, for which the system reached a maximum elasticity value. The viscous effect (imaginary elasticity) for the surface elasticity was estimated from the phase angle.

2.7. PM-IRRAS

Polarization-Modulated Infrared Reflection Absorption Spectroscopy (PM-IRRAS) was performed using a KSV PMI 550 instrument (KSV instrument Ltd, Helsinki, Finland). The Langmuir trough is set up so that the light beam reaches the monolayer at a fixed incidence angle of 80°. At this angle, the intensity is at maximum and the noise level is the lowest. The incoming light is continuously modulated between s- and p-polarization at a high frequency, which allows simultaneous measurements of the spectra for the two polarizations. From this, the differential reflectivity spectrum can be calculated [15], and a negative band indicates a transition moment oriented preferentially perpendicular to the surface, whereas a positive reflection absorption band indicates a transition moment oriented preferentially in the plane of the surface. The difference thus provides surface specific information, and the sum provides the reference spectrum. As the spectra are measured simultaneously, the effect of water vapor is reduced considerably.

3. Results and discussion

3.1. Obtaining active rPAC and its C-terminal truncated forms

The role played by the C-terminal end of pulchellin A-chain (PAC) in the protein–membrane interactions was assessed by creating three truncated forms of PAC which lack some (rPAC^{244} and rPAC^{239}) or all (rPAC^{236}) of the hydrophobic residues at the C-end of the protein (Fig. 1 — top). The C-terminus deletions were based on the alignment of several RIPs, including PAC and ricin A-chain (RTA) (Fig. 1 — bottom), which allowed us to confirm that the hydrophobic region was preserved. The heterologous expression of all constructs was achieved, making it possible to purify the truncated forms, as seen in Fig. 2. Significantly, after the *in vitro* depurination assay (Fig. S1), rPAC and its truncated forms were all catalytically active.

3.2. Interaction of the rPAC with lipid monolayers

The adsorption kinetics of rPAC and the two truncated forms (concentration of 40 ng mL^{-1}) on lipid monolayers were obtained at a low lipid packing (135 $Å^2$), at which the surface pressure is zero. Significant adsorption of the proteins onto DPPG (anionic) monolayers was observed, even at low surface packing, as indicated in Fig. 3A. It should be stressed that these proteins are not intrinsically surface active, and therefore the increase in surface pressure arises from the interaction with the lipid layer. It is likely that the presence of the monolayer at the air–water interface shifts the thermodynamic equilibrium in a way to cause a surface excess of the protein. Furthermore, the increase in pressure due to the adsorption of the proteins

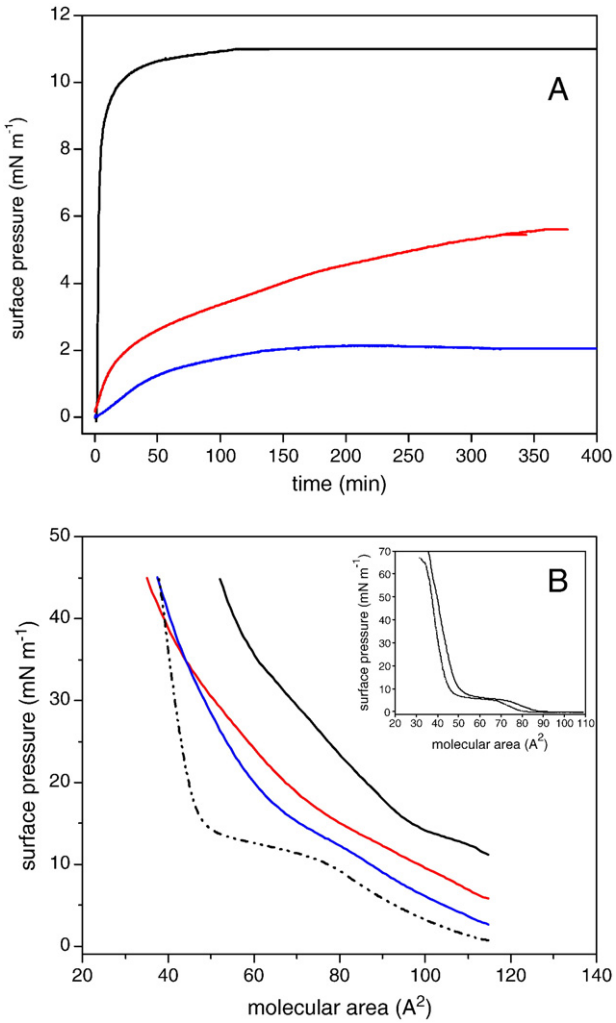

Fig. 3. (A) Adsorption kinetics for (—) rPAC, (—) rPAC^{244} and (—) rPAC^{239} on DPPG monolayers. (B) Surface pressure isotherms for DPPG monolayers in (·-·) phosphate buffer, (—) rPAC, (—) rPAC^{244}, (—) rPAC^{239} subphase. All proteins were at 40 ng mL^{-1} concentration. The inset in B corresponds to p-A isotherm for DPPC in (·-·) phosphate buffer, and in (—) rPAC solution, 40 ng mL^{-1}.

starts immediately after injection, indicating low diffusive effects. The change in surface pressure (Δπ) decreased as more amino acid residues were deleted from the C-terminus region of rPAC, in the following sequence for Δπ: rPAC > rPAC^{244} > rPAC^{239}. This is consistent with the C-terminus being the most hydrophobic region in the molecule; its deletion decreases the adsorption of the resulting polypeptide at the interface.

The interaction between rPAC and its truncated forms was much weaker with the zwitterionic DPPC monolayers, with a smaller adsorption for the same protein concentrations as for DPPG (results not shown). The higher interaction between rPAC and charged lipids is evident, even the C-terminus does not contain positively charged residues. Probably other characteristics of the DPPG lipid monolayer, such as hydration and fluidity, can contribute to increase the interaction between rPAC and the film. Day et al. [7], demonstrated with fluorescence spectroscopy and circular dichroism that the ricin A-chain altered the structure of PG vesicles, and this did not occur with PC vesicles. Similar results were reported for some type 1 RIPs composed only by the toxic A-chain and for trichosanthin, where the docking of the protein was stronger for charged membranes [16,17]. But the preferred interaction with charged membranes is not consensual in the literature, for RTA was found to fuse PC vesicles, thus altering their fluidity and T_m [18–22]. Therefore, it seems that the interaction between this class of proteins and lipids may depend on the protein and composition of the membrane.

As far as the present study is concerned, owing to the lower affinity of the protein for DPPC in Langmuir monolayers, we performed the subsequent experiments only with DPPG monolayers. Fig. 3B shows the π–A isotherms for DPPG obtained upon compressing the monolayer after the adsorption of the proteins had reached equilibrium. With the buffer used in the subphase, a neat DPPG monolayer displays a plateau at ~12 mN m^{-1}, characteristic of the coexistence of the liquid-expanded (LE) and liquid-condensed (LC) phases [23]. With the protein adsorption the π–A isotherms were shifted to larger areas in comparison to isotherm for neat DPPG. The shift followed the same sequence as in the adsorption kinetics, with rPAC inducing the largest expansion, followed by rPAC^{244} and rPAC^{239}. Note that at high surface pressure, *e.g.* 40 mN m^{-1} (higher than the membrane packing), both rPAC^{244} and rPAC^{239} were expelled from the interface, which can be inferred by the crossing point between their isotherm and the one for pure DPPG. For rPAC, on the other hand, even at high lipid packing, the shift was maintained, indicating that the protein remained in the lipid monolayer. Taken together, these results demonstrated the role of the C-terminal region in the incorporation of the protein into the membrane, since deletion in this portion decreased its interaction with lipid monolayers.

3.3. Investigating rPAC^{236} behavior with lipid monolayers

The adsorption kinetics of the protein with complete deletion in its C-terminal region, rPAC^{236}, was also investigated. Surprisingly, the increase in surface pressure induced by this truncated form was even higher than for the other forms (rPAC^{244} and rPAC^{239}), being almost the same as for the undeleted rPAC, as shown in Fig. 4A. Two hypotheses may be considered to explain this unexpected result. The first is that in the absence of the C-terminus, the interaction with other hydrophobic regions of the proteins becomes important. The second hypothesis is that the effects could be caused by destabilization of the proteins. This latter hypothesis would be consistent with Zhang et al. [24] who demonstrated that the deletion of the last seven amino acid residues from trichosanthin (type-1 RIP) C-terminal destabilized the tertiary structure of the protein, decreasing its cytotoxicity.

In order to verify which hypothesis is more probable, we performed additional experiments to check whether the deletion of the C-terminal, to built rPAC^{236}, altered its structure. Accordingly, we

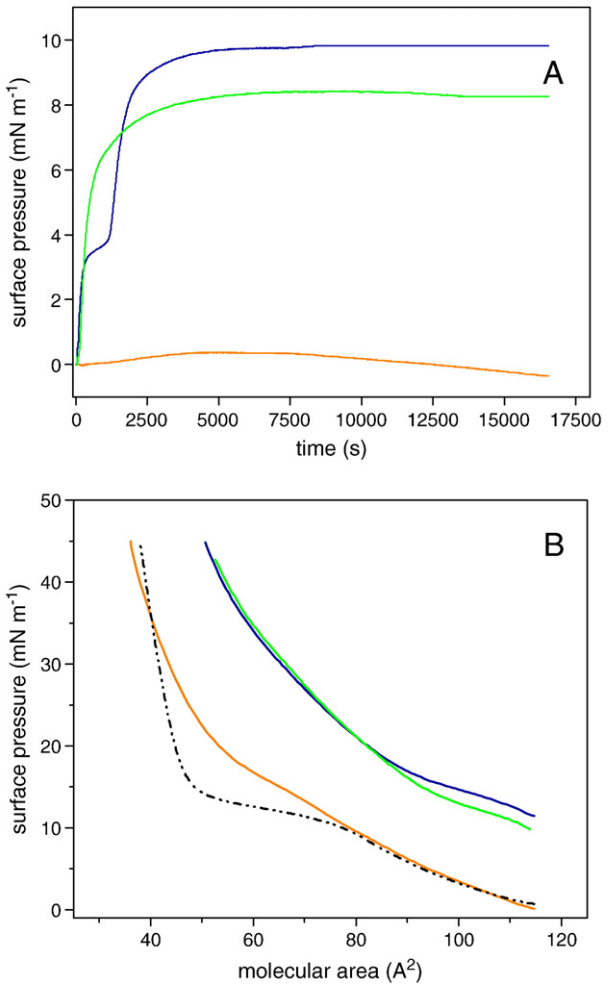

Fig. 4. (A) Adsorption kinetics for rPAC^{236} diluted (—), concentrated (—) and denaturated (—) proteins. (B) π–A isotherms for DPPG monolayers in:(···) buffer solution, rPAC^{236} diluted (—), concentrated (—) and denaturated (—) proteins. All proteins were at 40 ng mL^{-1} concentration.

manipulated the samples to obtain a denatured sample and an aggregated sample. The latter was obtained using a very concentrated stock solution of 0.5 mg mL^{-1}, which is much more concentrated than in the other experiments (0.02 mg mL^{-1}). In such high concentration, the protein is very unstable and some aggregates are commonly formed. The denatured sample was prepared by heating the solution until protein denaturing. As shown in Fig. 4A, adsorption of the denature sample was very small, probably because there was irreversible aggregation in the bulk of the solution. The aggregated sample, on the other hand, displayed a kinetic curve similar to rPAC^{236}, indicating that the protein can disaggregate when injected in the subphase, then interacting with the lipid monolayer. This disaggregation step may be inferred from the shoulder at π ~3.8 mN m^{-1} in Fig. 4A. The results in Fig. 4B for the surface pressure isotherms after the protein adsorption are consistent with the kinetic data. The isotherms were shifted to larger areas for rPAC^{236} and the aggregated sample, but no significant change was noted for the denatured rPAC^{236} sample.

It is therefore concluded that the interaction between rPAC^{236} and DPPG monolayers was not due to an artifact, since the CD spectra showing that the secondary structure of the proteins was not affected by the deletions, as will be commented upon below (Fig. 5). Hence, hypothesis 1 above, according to which other hydrophobic regions play a role, is the most likely. We shall return to this result and discuss its implications later on.

3.4. Mimicking the lipid packing of the biomembrane: surface elasticity measurements

The investigation of the rPAC C-terminus region with the biomembrane was complemented by measuring the adsorption kinetics for the proteins on DPPG monolayers at 30 mN m^{-1}, which correspond to the lipid packing in a biomembrane [14]. As for the experiments with zero initial π, the kinetics was followed by changes in π with time at a constant area, using the axisymmetric drop shape analysis. The adsorption kinetics at 30 mN m^{-1} was carried out for 40 min, and the changes in surface pressure (Δπ) are given in Table 1. The behavior with adsorption at high lipid packing was similar to that at low lipid packing, with effects in the order rPAC > rPAC ^{244} > rPAC^{239}. The ability of a protein to interact at this high lipid packing indicates that the polypeptide can be incorporated into the lipid layer, mainly by hydrophobic interactions with the lipid alkyl chains. This penetration into the monolayer decreased with the deletion, and rPAC^{239} was practically not incorporated into the membrane. Again, rPAC^{236} had strong interaction with the monolayer, with Δπ of 4.2 mN m^{-1}, which is higher than for rPAC^{244}, indicating the exposure and interaction of a great hydrophobic portion with the lipid layer.

After adsorption reached equilibrium, the mixed monolayer was disturbed with compression–expansion cycles to verify the stability of the interactions between proteins and the monolayer. Under these conditions, the parameter measured is the dilational surface elasticity (E), which brings information on how membrane fluidity is affected [13]. The results in Table 2 show that the incorporation of rPAC increased E to a value twice that of the pure lipid. The increase in E was ~47% and ~14% for rPAC^{244} and rPAC^{239}, respectively, again compared to neat DPPG. rPAC^{236} promoted an increase of 70% in E. These results indicate that all proteins affected the membrane fluidity, but at different extensions. In general, when a protein increases the elasticity, the monolayer becomes more structured. In several cases involving mixed proteins and lipid systems, the protein interacts not only with the lipid polar head but also with the hydrophobic tails [25] causing the monolayer to be more oriented. Consequently, the polypeptide moiety at the interface is able to compact the film, increasing the orientation of lipid chains, which may lead to an increase in surface elasticity. Therefore, the extent of penetration of the protein was also affected by the deletions in the C-terminal region.

3.5. Circular dichroism measurements

A-chains from type 2 RIPs are expected to alter the membrane fluidity. For instance, the ricin A-chain (RTA) strongly disturbed the lipid bilayer, resulting in membrane fusion and increasing the permeability [18,26]. Furthermore, the interaction of ricin A-chain with membranes was stronger than for holotoxin [20]. However, in addition to alterations in the packing of the lipids in different membrane models, some changes of the secondary structure of the protein can occur. For RTA, Day and coworkers verified that its interaction with POPG vesicles decreased its helix content from 35% to 32%, and increased in the β-sheet from 18% to 22% [7]. Mayerhofer and coworkers [10] found the insertion into membrane by RTA is a temperature-dependent process.

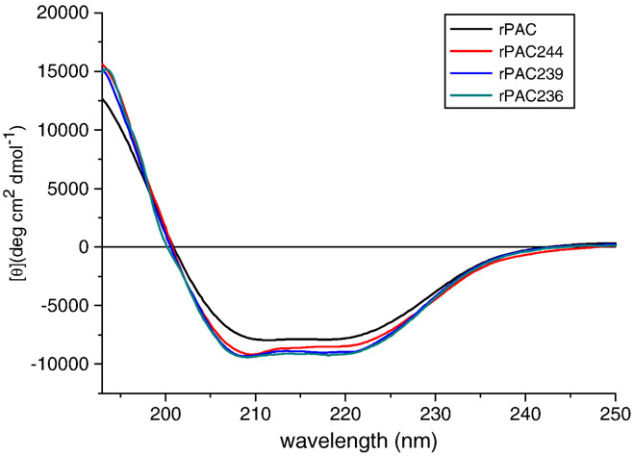

Fig. 5. CD spectra for (—) rPAC, (—) rPAC^{244}, (—) rPAC^{239}, and (—) rPAC^{236} incubated with vesicles at zero time. Protein concentration was 0.1 mg mL^{-1} obtained using a 0.1 cm path length cylindrical quartz cuvette.

Table 1
Changes (Δπ) in initial surface pressure of DPPG monolayer promoted by protein incorporation. The data were recorded after the surface pressure of equilibrium was reached.

Protein	Δπ (mN m^{-1}) (after 40 min)
rPAC	5.1
244	3.9
239	1.0
236	4.2

To verify if the secondary structure of rPACs was altered after interaction with DPPG, the proteins were incubated with DPPG vesicles for measuring circular dichroism. Taking into account the adsorption kinetics of the proteins onto DPPG monolayers, we tried to obtain various spectra as a function of time up to ~30 min, in which the system was near the equilibrium of adsorption. The results for the "time zero", immediately after incubation of rPAC or one of its truncated forms with DPPG vesicles, are shown in Fig. 5.

The spectra for rPAC and the mutants indicate that all proteins present similar structures with predominance of α-helix contents. Small differences in the intensity may be related to slight changes in secondary structure content of each protein, caused by deletions. Also, the CD spectra are identical to the case in which the proteins are not encapsulated in vesicles (results not shown). However, some minutes later (around 2 min.), the vesicles precipitated, making it difficult to draw conclusions. Probably, the proteins promoted the fusion/rupture of the vesicles, in agreement with previous reports in which toxic chains from RIPs were suggested to induce destabilization of the membrane [18,26].

Because CD spectroscopy was not able to provide evidence for alterations in the secondary structure of rPACs interacting with DPPG, we employed Polarization-Modulated Infrared Reflection Absorption Spectroscopy (PM-IRRAS) for Langmuir monolayers. This technique provides information on the molecular interaction and orientation at the membrane surface.

3.6. Secondary structure characterization by PM-IRRAS measurements

The PM-IRRAS spectra for rPAC–DPPG monolayers at distinct packing densities are shown in Fig. 6. Absorption bands were also observed in the 2800–3000 cm^{-1} region (not shown), assigned to C–H stretching for the alkyl chain of DPPG, but we shall focus on the amide bands region. Fig. 6A shows that the spectra do not change significantly with compression, which is explained by the stability of

Table 2
Dilational surface elasticity (E) for the DPPG–protein monolayers after adsorption kinetics at 30 mN m^{-1}.

Protein	E (mN m^{-1})
Pure DPPG	224.8
rPAC	475.5
244	330.9
239	258.5
236	382.7

protein conformation even at higher surface lipid packings. The bands at ~1500–1560 cm^{-1} are assigned to C–N or N–H stretching, being normally referred to as amide II. These bands are hard to assign because of interaction among the side chains [27]. The bands at 1600–1700 cm^{-1} are assigned to amide I (C═O stretching). The amide I intensities are affected in the spectra of Fig. 6A because of the negative band at ~1685 cm^{-1}, related to O–H bending of interfacial water [28]. Focusing on the region for amide I, we note the absence of bands related to α-helix structures, which should appear in the range 1649–1656 cm^{-1} [29]. The band at 1645 cm^{-1} can be assigned to disordered structures or β-turns [30], while the band at 1696 cm^{-1} is associated with anti-parallel β-sheets or β-turns [31]. One should recall that the CD spectra bring a global secondary structure of the protein, while PM-IRRAS is more sensitive to specific regions of the polypeptide chain interacting with the monolayer at the interface. Therefore, the PM-IRRAS data are more informative about the secondary structure of the C-terminal region interacting with DPPG.

Fig. 6B shows the PM-IRRAS spectra for rPAC adsorbed on a bare air–water interface. Although the protein presents low surface activity and there is no surface excess to decrease the surface tension of water, the molecules at the air–water interface can be detected by PM-IRRAS because they are anisotropic. The main feature of the spectrum is the presence of a strong positive band centered at 1654 cm^{-1}, which shows that most of the proteins remain as α-helix, as observed in the CD spectra. Also, the amide I/amide II intensity ratio, which is related to the order parameter [32], is inverted, with amide I displaying higher intensities. For the DPPG–rPAC monolayer, the amide I/amide II ratio is below one, which means that the transition dipole moment of amide II is more preferentially oriented along the interface plane than that of the amide I mode [32]. Therefore, the association of rPAC with the negative charged monolayer resulted in a structural change, suggesting the exposure of an unordered region.

Fig. 7 indicates that $rPAC^{236}$ presents α-helix as its main secondary structure when adsorbed at a bare air–water interface since a prominent band appears at 1651 cm^{-1}. The band at 1692 cm^{-1} represents the fractions of the polypeptide with disordered secondary structure. However, in contrast to the behavior of rPAC, its structure was roughly kept upon interaction with DPPG, since the strong band at 1651 cm^{-1} was preserved. Other structures are changed, such as the bands at 1622 cm^{-1}, and 1671 cm^{-1}, attributed respectively to β-sheets and β-turns, which appears for the DPPG–protein spectra and not for the pure protein. This means that some β-sheet structures are also detected upon interaction with DPPG. Also, for $rPAC^{236}$ there is no indication of unordered band, the amide I/amide II is kept higher than unity, and at ~1645 cm^{-1} there is no evidence of a band, usually related to unfolded structures [33]. The band at 1559 cm^{-1} is the amide II band, and its relatively low intensity, in comparison to amide I bands, indicates that most of the adsorbed proteins have their secondary structure preserved.

It was concluded that the insertion of rPAC into the membrane requires exposure of the C-terminal region to better adapt to the hydrophobic environment provided by the lipid monolayer. Considering the unordered folded of the C-terminal region, obtained from high resolution crystallographic data of the protein [34] (represented in blue in Fig. 8), one may infer that the interaction of pulchellin A-chain with DPPG – taken as a model for the ER membrane – is a

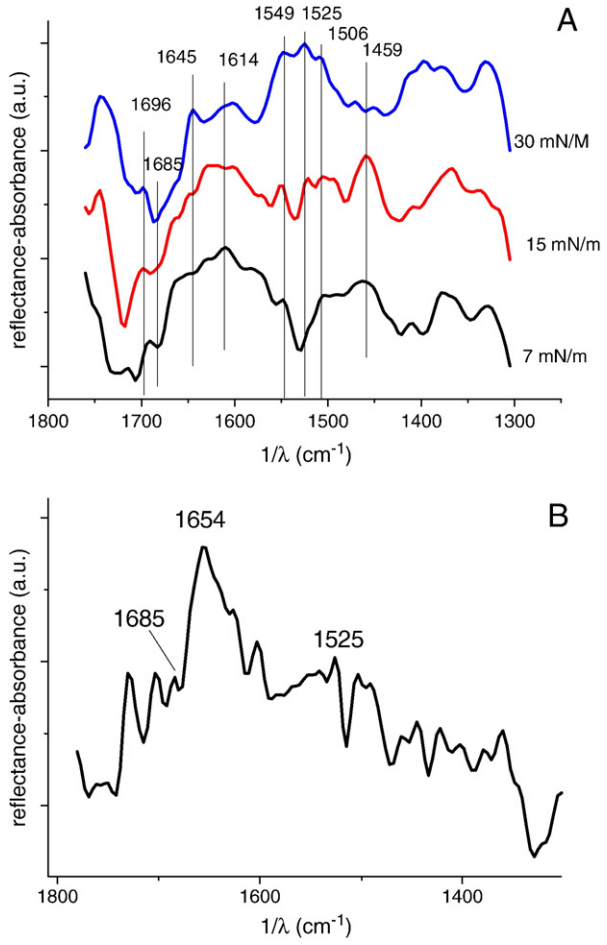

Fig. 6. (A) PM-IRRAS spectra for DPPG–rPAC mixed monolayers at three different surface pressures, as indicated in the graph. (B) PM-IRRAS spectrum for rPAC adsorbed at the air–water interface at null surface pressure (no surface excess).

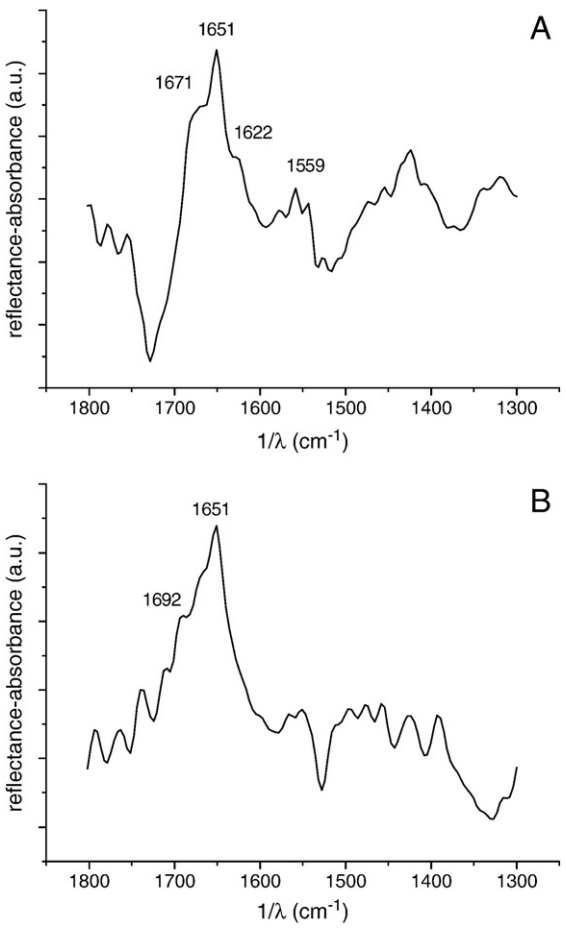

Fig. 7. (A) PM-IRRAS spectra for DPPG–$rPAC^{236}$ mixed monolayers at $\pi = 30$ mN m^{-1}. (B) PM-IRRAS spectrum for rPAC localized at the air–water interface.

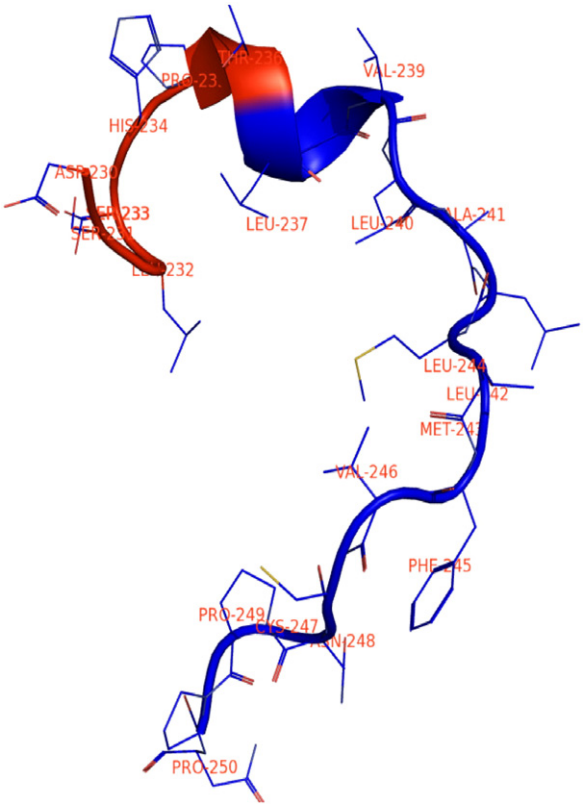

Fig. 8. C-terminal region of rPAC (residues 236–251, in blue) analyzed in this report. Note that the hydrophobic residues in it adopt an unordered fold. Some of its neighboring residues are shown (residues 225–235, in red). C-terminal was obtained from the recently solved crystal structure of pulchellin [34] and manipulated with Pymol software.

necessary step for the protein to be recognized by ERAD, since this interaction results in a less folded region (unordered). The ability in promoting a local structural transition seems to be depleted with successive deletion of amino acid residues from C-terminal. This is supported by the decreasing surface activities of the successive fractions of the protein with residues deletion. However, for the rPAC^{236}, where a highest extent of C-terminus was removed, the surface activity was more significant, thus implying in another mechanism of interaction with the membrane. In fact, the data from PM-IRRAS spectroscopy indicated no adsorption of unordered structures. Thus, the change in structuring of rPAC^{236}, even before interaction with DPPG, may provide a higher exposure of other hydrophobic regions. Upon examining Fig. 8, the region penetrating into the membrane should comprise other α-helix region exposed after the C-terminal deletion, but we cannot precise exactly where is this α-helix in the structure of the protein. Indeed, the band at 1671 cm^{-1} assigned to β-turns appears only in rPAC^{236} interacting with DPPG, which implies in different alternatives for rPAC^{236} to expose other hydrophobic groups rather than the C-terminus.

4. Conclusions

We demonstrated that rPAC interacts with Langmuir monolayers of DPPG, as well as its three C-terminal truncated forms. The extension of the adsorption of the proteins with the lipid films follows the sequence of C-terminal deletion, but rPAC^{236} protein presented an anomalous behavior, which was proven not to be an artifact. Dilational surface elasticity data demonstrated that all proteins affect the fluidity of the model membrane indicating incorporation onto the interfacial film. With CD measurements it was not possible to verify changes in the secondary structure of the protein, since the vesicles precipitated in less than 5 min of incubation. This indicates that the proteins probably destabilize the bilayer membrane. Using PM-IRRAS technique for Langmuir monolayers, we noted that the α-helix contribution from rPAC with its C-terminal region intact, present for the protein in solution, disappeared when the protein was in contact with the DPPG film. Instead, mainly unordered structures were observed. This finding is consistent with the insertion being a fundamental step for the protein to be recognized as an ERAD substrate. Taken together, the results give strong support to the idea that the hydrophobic path in the C-terminal region plays a vital role in insertion of rPAC into biomembranes. The restructuring after membrane insertion is believed to be the signaling step for the protein to be recognized by ERAD machinery and finally reach the ribosome to develop its toxic activity.

Supplementary materials related to this article can be found online at doi:10.1016/j.bbamem.2011.10.002.

Acknowledgements

This work was supported by FAPESP and CNPq.

References

[1] A.L.C. Silva, A.C.G. Horta, R.A. Moreira, L.M. Beltramini, A.P.U. Araujo, Production of *Abrus pulchellus* ribosome-inactivating protein from seeds callus culture, Toxicon 41 (2003) 841–849.
[2] A.L.C. Silva, L.S. Goto, A.R. Dinarte, D. Hansen, R.A. Moreira, L.M. Beltramini, A.P.U. Araujo, Pulchellin, a highly toxic type 2 ribosome-inactivating protein from *Abrus pulchellus* — cloning, heterologous expression of A-chain and structural studies, FEBS J. 272 (2005) 1201–1210.
[3] L.S. Goto, P.V. Castilho, M.R. Cominetti, H.S. Selistre-Araujo, A.P.U. Araujo, Endocytosis of pulchellin and its recombinant B-chain into K-562 cells: binding and uptake studies, BBA-Gen. Subj. 1770 (2007) 1660–1666.
[4] P.V. Castilho, L.S. Goto, L.M. Roberts, A.P.U. Araujo, Isolation and characterization of four type 2 ribosome inactivating pulchellin isoforms from *Abrus pulchellus* seeds, FEBS J. 275 (2008) 948–959.
[5] B. van Deurs, O.W. Petersen, S. Olsnes, K. Sandvig, The ways of endocytosis, Int. Rev. Cytol. 117 (1989) 131–177.
[6] L.M. Roberts, J.M. Lord, Ribosome-inactivating proteins: entry into mammalian cells and intracellular routing, Mini Rev. Med. Chem. 4 (2004) 505–512.
[7] P.J. Day, T.J.T. Pinheiro, L.M. Roberts, J.M. Lord, Binding of ricin A-chain to negatively charged phospholipid vesicles leads to protein structural changes and destabilizes the lipid bilayer, Biochemistry 41 (2002) 2836–2843.
[8] J.C. Simpson, J.M. Lord, L.M. Roberts, Point mutations in the hydrophobic C-terminal region of ricin-a chain indicate that Pro250 plays a key role in membrane translocation, Eur. J. Biochem. 232 (1995) 458–463.
[9] M.L. Suhan, C.J. Hovde, Disruption of an internal membrane-spanning region in Shiga toxin 1 reduces cytotoxicity, Infect. Immun. 66 (1998) 5252–5259.
[10] P.U. Mayerhofer, J.P. Cook, J. Wahlman, T.T.J. Pinheiro, K.A.H. Moore, J.M. Lord, A.E. Johnson, L.M. Roberts, Ricin A chain insertion into endoplasmic reticulum membranes is triggered by a temperature increase to 37 degrees C, J. Biol. Chem. 284 (2009) 10232–10242.
[11] U.K. Laemmli, Cleavage of structural proteins during the assembly of the head of bacteriophage T4, Nature 227 (1970) 680–685.
[12] Y. Endo, K. Mitsui, M. Motizuki, K. Tsurugi, The mechanism of action of ricin and related toxic lectins on eukaryotic ribosomes — the site and the characteristics of the modification in 28-S ribosomal-Rna caused by the toxins, J. Biol. Chem. 262 (1987) 5908–5912.
[13] T.M. Nobre, F.J. Pavinatto, M.R. Cominetti, H.S. Selistre de-Araujo, M.E.D. Zaniquelli, L.M. Beltramini, The specificity of frutalin lectin using biomembrane models, BBA-Biomembranes 1798 (2010) 1547–1555.
[14] D. Marsh, Lateral pressure in membranes, BBA-Rev. Biomembr. 1286 (1996) 183–223.
[15] F.J. Pavinatto, C.P. Pacholatti, E.A. Montanha, L. Caseli, H.S. Silva, P.B. Miranda, T. Viitala, O.N. Oliveira, Cholesterol mediates chitosan activity on phospholipid monolayers and Langmuir–Blodgett films, Langmuir 25 (2009) 10051–10061.
[16] R.A. Demel, Y. London, W.S. Geurtsva, F.G. Vossenbe, L.L. Vandeene, Specific interaction of myelin basic protein with lipids at air–water interface, Biochim. Biophys. Acta 311 (1973) 507–519.
[17] X.F. Xia, F. Wang, S.F. Sui, Effect of phospholipid on trichosanthin adsorption at the air–water interface, BBA-Biomembranes 1515 (2001) 1–11.
[18] T. Utsumi, A. Ide, G. Funatsu, Ricin-A-chain induces fusion of small unilamellar vesicles at neutral pH, FEBS Lett. 242 (1989) 255–258.
[19] P. Pohl, Y.N. Antonenko, V.Y. Evtodienko, E.E. Pohl, S.M. Saparov, I.I. Agapov, A.G. Tonevitsky, Membrane fusion mediated by ricin and viscumin, BBA-Biomembranes 1371 (1998) 11–16.

[20] T.S. Ramalingam, P.K. Das, S.K. Podder, Ricin-membrane interaction — membrane penetration depth by fluorescence quenching and resonance energy-transfer, Biochemistry 33 (1994) 12247–12254.
[21] A. Menikh, M.T. Saleh, J. Gariepy, J.M. Boggs, Orientation in lipid bilayers of a synthetic peptide representing the C-terminus of the A(1) domain of shiga toxin. A polarized ATR-FTIR study, Biochemistry 36 (1997) 15865–15872.
[22] M. Picquart, E. Nicolas, F. Lavialle, Membrane-damaging action of ricin on DPPC and DPPC-cerebrosides assemblies — a Raman and FTIR analysis, Eur. Biophys. J. Biophys. 17 (1989) 143–149.
[23] D. Grigoriev, R. Krustev, R. Miller, U. Pison, Effect of monovalent ions on the monolayers phase behavior of the charged lipid DPPG, J. Phys. Chem. B 103 (1999) 1013–1018.
[24] F. Zhang, Y.J. Lu, P.C. Shaw, S.F. Sui, Change in pH-dependent membrane insertion characteristics of trichosanthin caused by deletion of its last seven C-terminal amino acid residues, Biochem. Mosc. 68 (2003) 436–445.
[25] T.F. Schmidt, L. Caseli, T.M. Nobre, M.E.D. Zaniquelli, O.N. Oliveira, Interaction of horseradish peroxidase with Langmuir monolayers of phospholipids, Colloids Surf. A 321 (2008) 206–210.
[26] T. Utsumi, Y. Aizono, G. Funatsu, Interaction of ricin and its constituent polypeptides with dipalmitoylphosphatidylcholine vesicles, Biochim. Biophys. Acta 772 (1984) 202–208.
[27] L. Caseli, M.L. Moraes, V. Zucolotto, M. Ferreira, T.M. Nobre, M.E.D. Zaniquelli, U.P. Rodrigues, O.N. Oliveira, Fabrication of phytic acid sensor based on mixed phytase-lipid Langmuir–Blodgett films, Langmuir 22 (2006) 8501–8508.
[28] J. Orbulescu, M. Micic, M. Ensor, S. Trajkovic, S. Daunert, R.M. Leblanc, Human cardiac troponin I: a Langmuir monolayer study, Langmuir 26 (2010) 3268–3274.
[29] W.P. Ulrich, H. Vogel, Polarization-modulated FTIR spectroscopy of lipid/gramicidin monolayers at the water interface, Biophys. J. 76 (1999) 1639–1647.
[30] I. Cornut, B. Desbat, J.M. Turiet, J. Dufourcq, In situ study by polarization modulated Fourier transform infrared spectroscopy of the structure and orientation of lipids and amphipathic peptides at the air–water interface, Biophys. J. 70 (1996) 305–312.
[31] A. Haouz, C. Twist, C. Zentz, P. Tauc, B. Alpert, Dynamic and structural properties of glucose oxidase enzyme, Eur. Biophys. J. Biophys. 27 (1998) 19–25.
[32] A. Dhathathreyan, U. Baumann, A. Muller, D. Mobius, Characterization of complex gramicidin monolayers by light-reflection and Fourier-transform infrared-spectroscopy, Biochim. Biophys. Acta 944 (1988) 265–272.
[33] H. Lavoie, D. Blaudez, D. Vaknin, B. Desbat, B.M. Ocko, C. Salesse, Spectroscopic [correction of eSpectroscopic] and structural properties of valine gramicidin A in monolayers at the air-water interface, Biophys. J. 83 (2002) 3558–3569.
[34] P.V. Castilho, A.P.U. Araujo, M.V.A.S. Navarro, unpublished results.